Conference Paper, Published Version

Hein, Sebastian; Winter, Christian

Video Monitoring of Beach States, Coastline Migration and Beach Nourishments – A Case Study from Sylt Island, North Sea

Coastal Structures 2019 - Nils Goseberg, Torsten Schlurmann (eds) - © 2019 Bundesanstalt für Wasserbau
ISBN 978-3-939230-64-9 (Online) - DOI: 10.18451/978-3-939230-64-9_082

Video Monitoring of Beach States, Coastline Migration and Beach Nourishments – A Case Study from Sylt Island, North Sea

S. S. V. Hein
HPA Hamburg Port Authority, Hamburg, Germany
C. Winter
Institute of Geosciences, Christian-Albrechts Universität zu Kiel, Kiel, Germany

Abstract: This study explores the cost-effective method of video monitoring to observe coastline migration and evaluates a beach nourishment, undertaken in May 2017 at the intermediate beach Bunker Hill on Sylt island, in the south-eastern North Sea. Daily coastlines at mean water level and 1 m below were derived from photogrammetry for a period from January to October 2017. Seasonal coastline migrations of up to 22 m and distinct seasonal beach state transformations were detected. Seasonal rip channel and bar migrations are up to 100-200 m southward in spring and northward in autumn. A beach nourishment was observed, in terms of initial beach broadening of 31 m, sand redistribution to a new equilibrium state until end of June and finally the erosion due to storm Xavier in the beginning of October. This study shows how well natural morphology variations and beach nourishments can be monitored over long-time durations of several seasons, with resolutions that can keep up with costly and time-consuming alternative measuring campaigns.

Keywords: Beach cameras, beach dynamics, beach state, coastline migration, nourishments, storm impact

1 Introduction

Coasts and especially sandy beaches belong to the most dynamic regions on earth (Woodroffe 2002). At these buffer zones between sea and land terrestrial, marine and atmospheric processes meet, accompanied by an intensive anthropogenic influence. Rising sea levels and increasing intensities and frequencies of storm events likely further enforce beach erosion.

Besides a variety of hard-engineering measures, such as concrete walls, soft-engineering provides alternative approaches to cope with beach erosion. The latter measures are often favoured, as they are more compatible with touristic and ecological interests. Beach nourishments have become a popular and proven method in Europe over the last decades. Since 1972, on average more than 1 million m³ of sand at a cost of more than 180 million euros have been replaced at Sylt's west coast. These actions are necessary to rebalance the beach erosion induced by the high energetic wave climate in the German Bight (Richter et al. 2013). Monitoring such nourishments is commonly very expensive and time consuming using traditional terrestrial or airborne methods. Consequently, the resolution in space and time is cost limited. But a frequently observation is necessary for monitoring highly dynamic morphology changes, to assign them to events and to evaluate coastal protection measures such as sand nourishments.

An alternative, which came up in the 1980s and have been steadily developed further ever since, is the video monitoring approach (Smith & Bryan 2007; Blossier et al. 2017a). It is more economical, because nearly no costly manpower is needed. The method allows also for a high resolution in the time domain as well as spatial over long durations (e.g. in this study over 304 days), being thus well qualified for monitoring coastal morphodynamics. The spatial resolution can reach as high as a few decimetres near the camera to a few metres in a kilometre distance, while vertical accuracy is above

10 cm (Blossier et al. 2017a). This resolution excels most of the other airborne and terrestrial methods, allowing for live monitoring even small-area morphology changes.

We used the video monitoring method to observe the natural coastline migration and to evaluate a beach nourishment, undertaken from the 7th until the 13th of May 2017 at the intermediate Bunker Hill beach on Sylt island.

2 Study Area and Methods

The present study was carried out at Bunker Hill beach, Sylt island, one of the North Frisian barrier islands located in the German Bight, North Sea (Fig. 1). Bunker Hill beach is a steep sloping sandy beach (medium to coarse sand) which generally exhibits a double-barred profile with semi-diurnal tides ranging around 2 m (Blossier et al. 2017a). Waves are generated from westerly winds, mainly between 247.5° and 315°, with highest waves from the North West. Mean significant wave heights at the offshore buoy Westerland are fluctuating around one metre, maximum significant wave heights can exceed 5.1 m with wave periods generally between 3 s to 8 s (Federal Maritime and Hydrographic Agency (BSH) 2019).

The monitored beach site covers an area of 200 m by 1150 m (UTM32: 453704 to 453905 easting, 6072900 to 6071750 northing). It was observed by two Lumenera Le 375CP cameras with 3.1-megapixel CMOS-Sensors, at a resolution of 2048 x 1536 pixels and a frame rate of 10 fps. The cameras were equipped with Fujinon lenses with a focal length of 16 mm. They were positioned 25 m above mean water level (MWL). Ten-minute time-exposure-pictures were used, thus single wave and wave group induced wave set-up and swash dynamics are neglected.

The pictures were rectified to a planar top view (Fig. 2). The necessary intrinsic camera parameters were determined by the chessboard-method (Heikkila and Silven 1997). Extrinsic parameters were achieved by the interpolation technique of Ground Control Points (GCP), determined using RTK-GPS. For the N-viewing camera 17 GCPs were used and 22 GCPs were used for the NW-viewing camera.

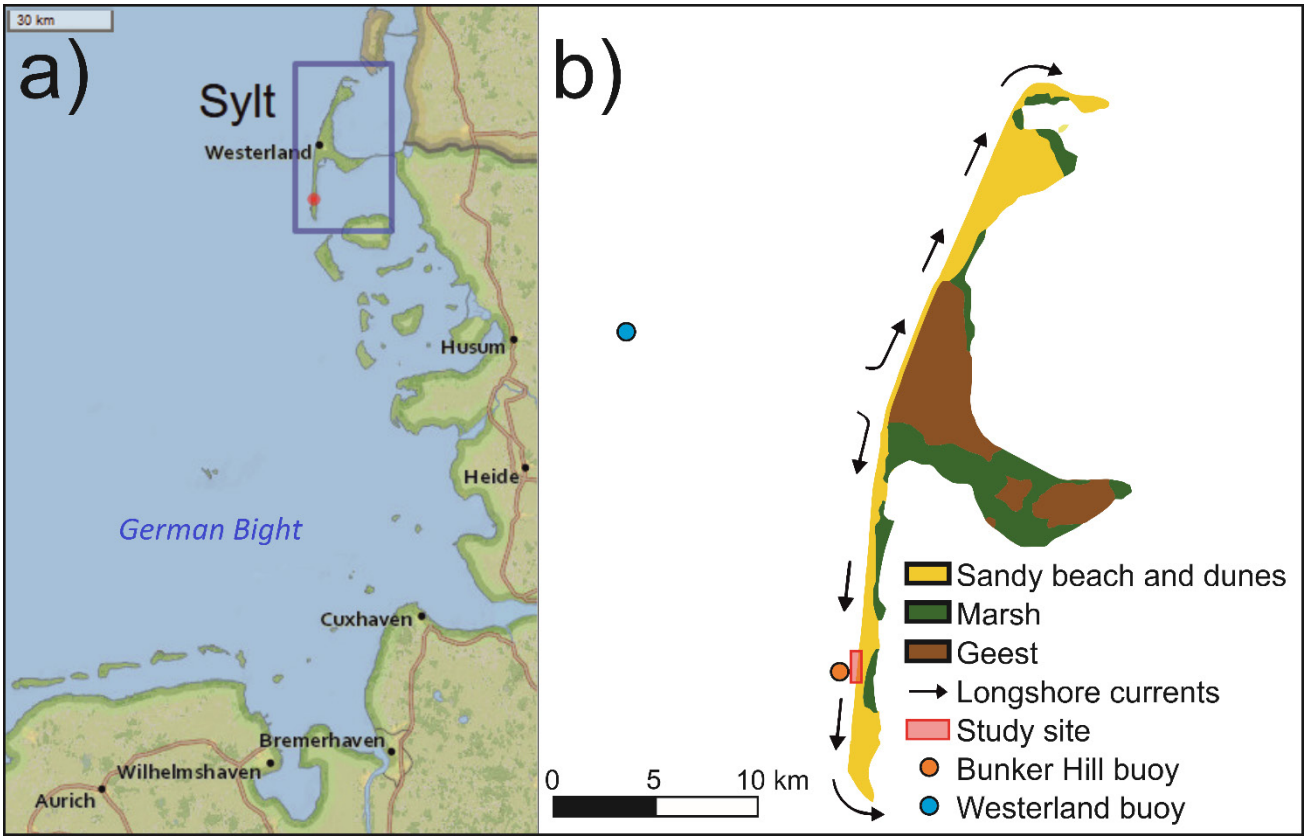

Fig. 1. a) Geographical setting of the study site indicated by the red point. Underlying map derived from mapmaker.nationalgeographic.org (2019). b) Geology of the North Frisian island Sylt and commonly assumed longshore current pattern after Klatt (2013).

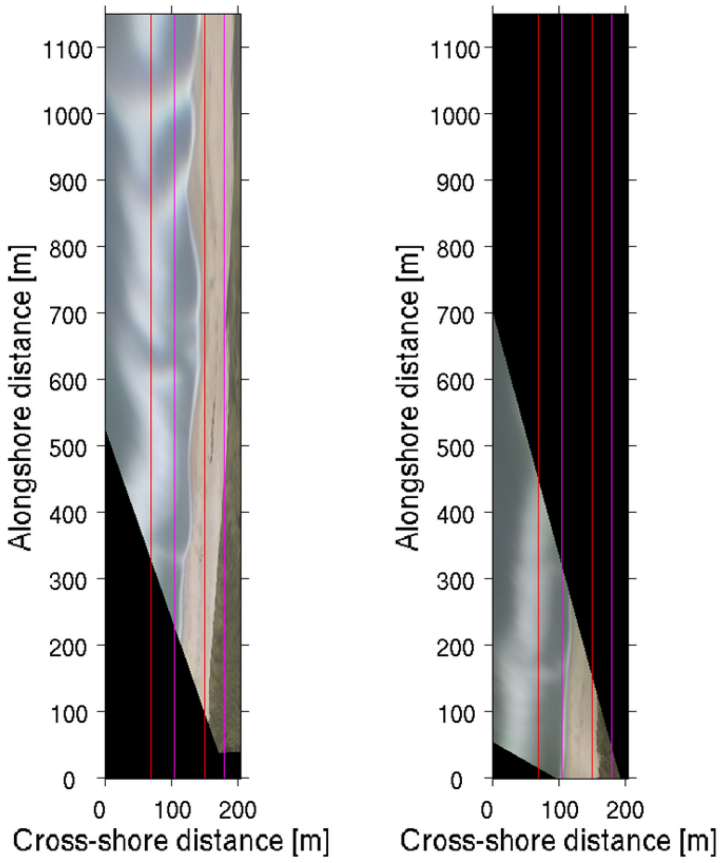

Fig. 2. Examples of rectified pictures from the N-camera (left) and the NW-camera (right). Magenta/red lines show the predefined searching area for the automatic coastline detection for January to April (magenta) and May to October (red).

The metre-per-pixel resolution was set to 0.3 m in N-S and W-E directions. Because of the central perspective, the accuracy decreases with distance. The N-S accuracy at the distant north end amounts to ca. 10 m while the W-E accuracy stays below 1 m.

The water levels assigned to the pictures are derived from the tide gauge at Hörnum harbour (South Sylt, data provided by the BSH), considering a 14 min phase difference between Bunker Hill beach and the tide gauge. Outliers were replaced by interpolating between adjacent values. Additionally, wave climate data, such as the significant wave height and the wave directions were supplied by the BSH.

For almost all days from 1st of January to the 28th of October one picture at MWL ±0.1 m was picked from both cameras for the coastline determination. Beginning from May, we chose an additional daily picture at 1 m below MWL, for a better evaluation of the beach nourishment. The coastlines were determined after Smith and Bryan (2007), using the blue-to-red ratios of pixels. If the difference of this ratio between two pixels, adjacent in W-E direction, exceeded a critical threshold, the coastline position was set. Critical thresholds of ratios (T_{crit}) were set to

$$T_{crit} = mean\_ratio_{sea} + 0.5 \cdot (mean\_ratio_{beach} - mean\_ratio_{sea}) \quad (1)$$

or

$$T_{crit} = 0.7 \cdot mean\_ratio_{beach} + 0.3 \cdot mean\_ratio_{sea} \quad (2)$$

depending on light and weather conditions. To speed up the coastline detection, a 250 m wide searching area for January to April and a 270 m wide area for May to October were pre-defined (Fig. 2). If the conditions did not allow an automatic coastline determination or if a visual control revealed divergences between automatically determined and real coastlines, the coastlines were manually traced.

Between the 7th and the 11th of May a beach nourishment was carried out. The determined coastline displacements due to the nourishment were evaluated via a comparison with terrestrial surveys of the 3rd and 17th of May, undertaken by the Agency for Coastal Defence, National Park and Marine Conservation Schleswig-Holstein (LKN).

Video monitoring is subject to natural restrictions, influencing the picture quality. Obviously, monitoring is limited to daylight hours. Furthermore, light reflexions on the sea surface as well as sunrise and sunset induced red-colouring lead next to bad weather influences to uselessness of pictures (Fig. 3). The maximal error of coastline positioning in the N-camera area is 1.5 m and 6.2 m in the NW-camera zone. The main possible cause for errors is the inaccuracy of the assigned sea levels, as they were not measured at place. The tidal curves differ between Bunker Hill beach and Hörnum harbour. For example, even so the tide at Bunker Hill beach show an average 14 min delay in comparison to Hörnum harbour, wave and wind driven alterations may influence the timing, height and duration of individual tidal cycles.

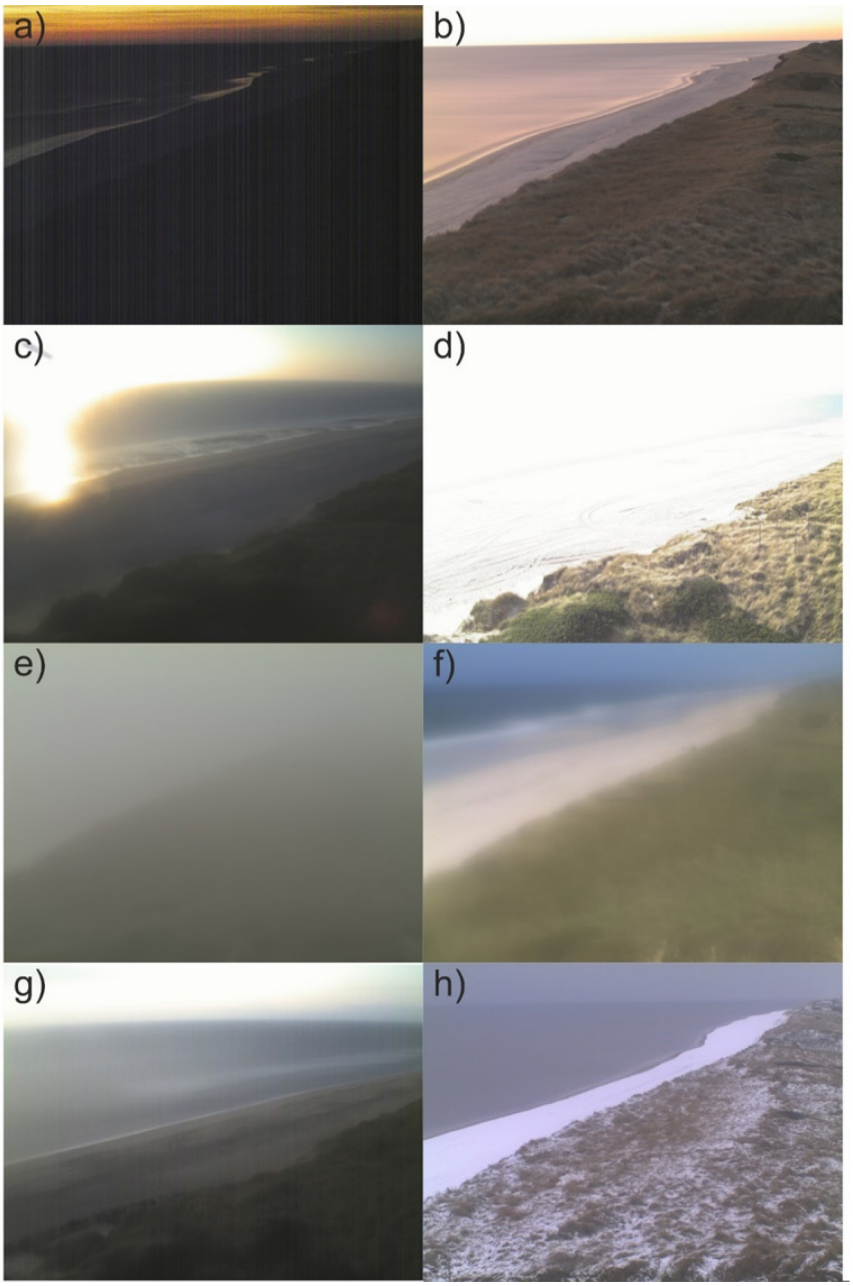

Fig. 3. Light (a-d) and weather (e-h) induced quality impairments of the video material, resulting in not automatically or not at all detectable coastlines. a) Underexposure b) Dusk and dawn induced red colouring c) Light reflexion d) overexposure e) fog f) wetted lens g) dark colouring of wet sand h) white colouring due to snow.

3 Results

3.1 Seasonal Morphology Changes

To investigate the natural seasonal changes, not the whole observation area was included in the analysis, but solely the northernmost part between 730 m and 1150 m north of the camera system. This part is 250 m northward of the nourished part of the beach, which is located in the southernmost 480 m of the observation area (Fig. 2). The northernmost part of the observation area was unlikely affected by the nourishment, as the coast parallel currents and potential transport pathways have a southward direction (Tillmann and Wunderlich 2014). The average daily coastline positions show a significant beach broadening in the second half of April. The distance between the most landward and seaward averaged coastline position from January until October was 22.2 m (Fig. 4). The averaged seasonal coastline positions (Tab. 1) show that the spring and summer beach was on average up to 6.4 m broader than the winter beach. The month with the most seaward averaged coastline position was May with 7.1 m seaward of the all-time mean position.

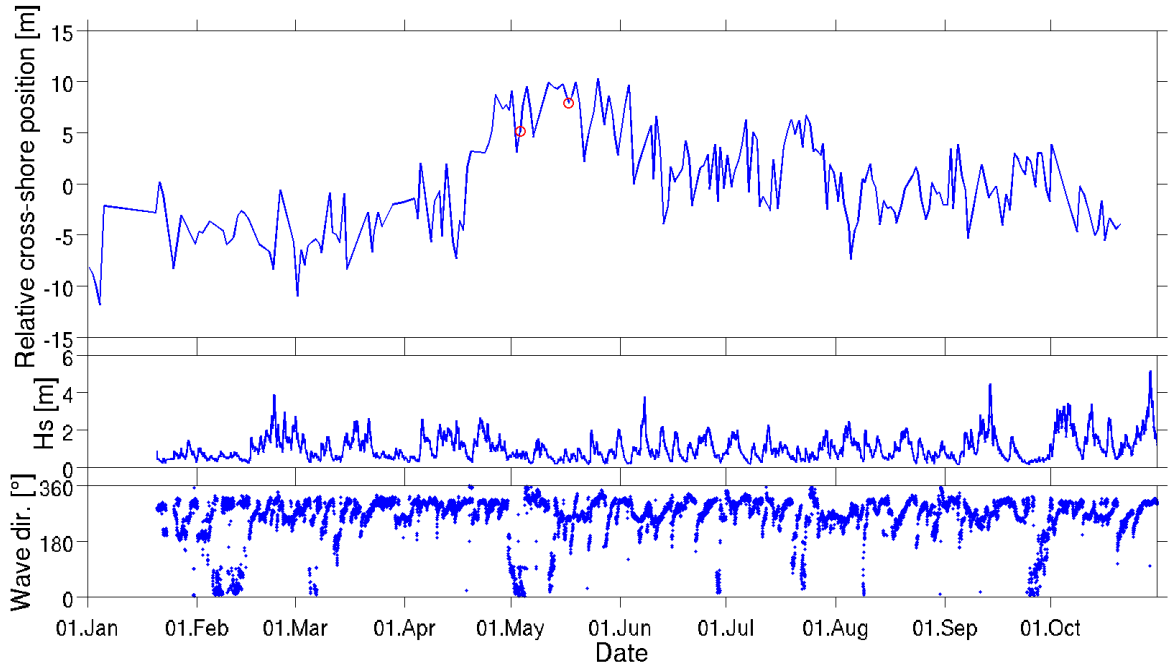

Fig. 4. Averaged coastline positions of the most northern part of the observed beach (730-1150 m north from the camera system). Values are plotted in relation to the all-time mean position. Red circles: Dates of the terrestrial topography measurements. Additionally shown are the significant wave height and mean direction of incoming waves, measured at the Westerland buoy (BSH).

Tab. 1. Monthly and seasonal averaged coastline positions of the most northern part of the observed beach (730-1150 m north from the camera system) in comparison to the all-time mean.

Month	Coast Position	Season	Coast Position
Jan	-5.7	Winter	-5.1
Feb	-4.3		
Mar	-5.0		
Apr	0.6	Spring	1.3
May	7.1		
Jun	2.0		
Jul	2.6	Summer	0.9
Aug	-1.6		
Sep	0.1	Autumn	-0.8
Oct	-2.6		

The coastline positions of the 0.3 m long beach sections show a change from a weak undulation in January and February to a more pronounced undulation appearing from spring until the end of

October with peak-to-valley values of up to 25 m (Fig. 5). This goes along with a change of the bars from long coast parallel sandbars to separated sandbars, divided by southward skewed rip current channels (Fig. 6).

Furthermore, the rip channels and aligned embayments of the beach face show a 100-200 m southward migration and fusions of beach horns in April. From mid-September, a reversed migration is indicated.

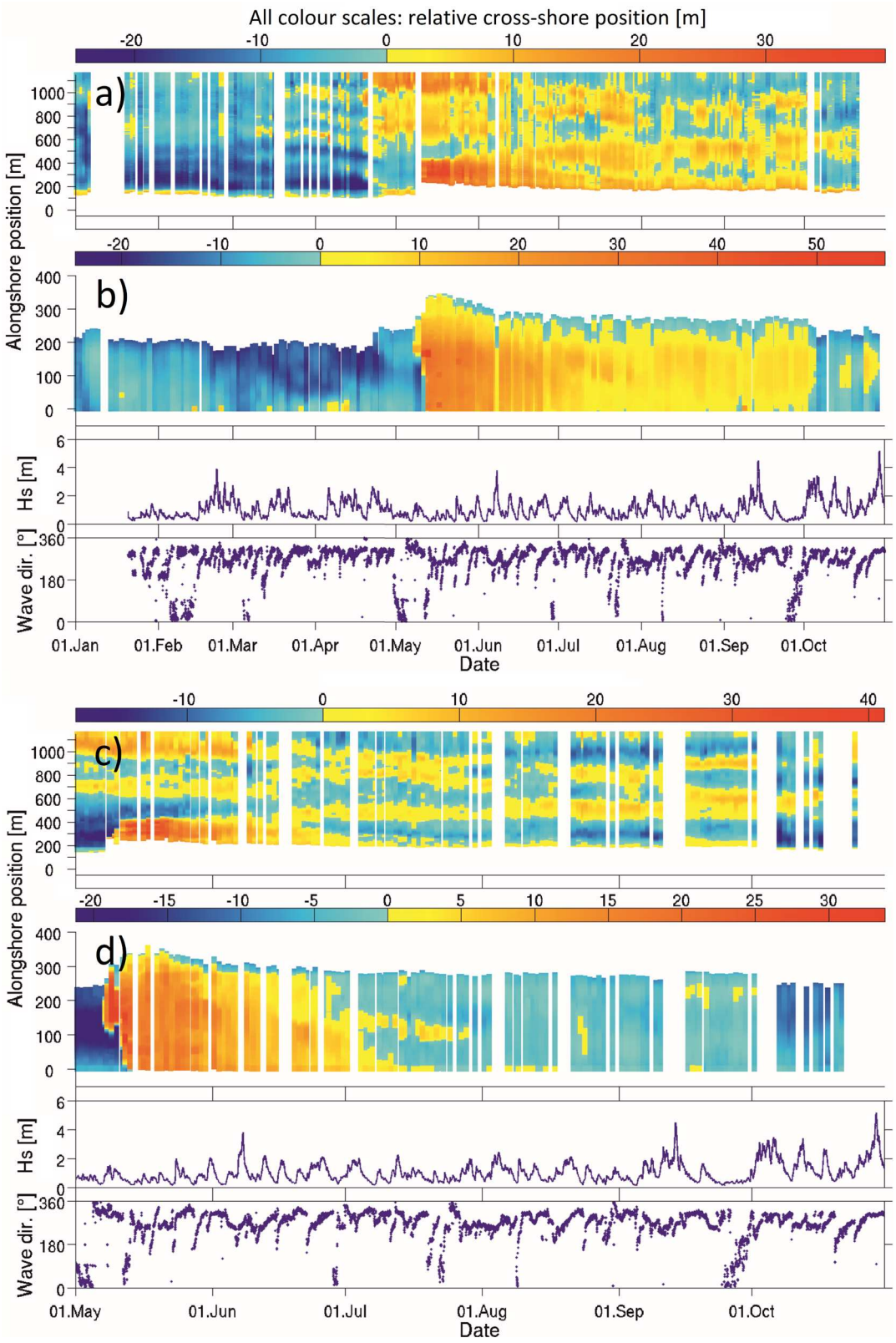

Fig. 5. Relative cross-shore coastline positions, indicated by the colour scales, are plotted in relation to their 0.3 m long beach section specific all-time mean. Positive values indicate seaward positions. Shown are the coastline positions at mean water level of a) the N-camera and b) NW-camera zone as well as 1 m below mean water level of c) the N-camera and d) the NW-camera. Additionally shown are the significant wave height and mean direction of incoming waves, measured at the Westerland buoy (BSH).

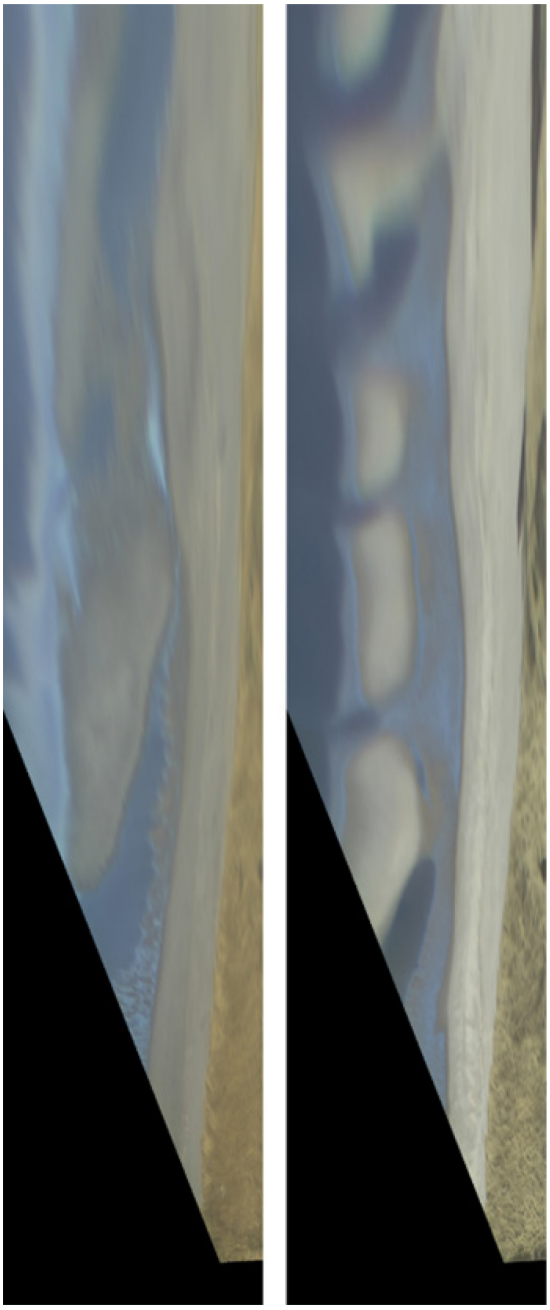

Fig. 6. Left: Continuous coast parallel sandbar at the 5th of January. Right: Fragmented sandbars divided by skewed rip current channels at the 30th of April.

3.2 Beach Nourishment Observations

Between the 07th and 13th of March, a 467 m beach transect in the most southern 480 m of the observed beach was nourished with 72,490 m³ sand (LKN, pers. communication). As the terrestrial pre- and post-morphology-measurements took place on the 3rd and 17th, those dates are used as reference. To include the coast parallel sand spreading over time, a 250 m long beach section north of the initial nourished area was included in the evaluation, because although the main part of the sand spread southward, a smaller part also spread northward. The initial beach broadening amounted to 32 m in the NW-camera zone from 0 to 480 m, and 17 m (20 m at MWL-1 m) in the N-camera zone between 100 to 730 m (Fig. 7). The broadening at 1 m below MWL was greater, as the MWL coastlines already retreated between the 13th and 17th while the low water level coastlines migrated further seawards (Fig. 5). Until mid-July the averaged coastlines retreated 10 m in the southern N-camera zone and 20 m in the NW-camera zone. At the same time, the supplied sand body spread 200 m to the north. From end of June, an embayment developed between the 350 m and 450 m north of the cameras, separating the spread sand body. Southward spreading also occurred but was not visually covered and can thus not be quantified. The new coastline just showed minor changes until

end of September. In comparison to the pre-nourishment state, the newly formed MWL coastlines were 10 m seaward in the NW-camera zone and 7 m in the N-camera zone. The coastlines at 1 m below MWL were even 10 and 13 m seaward, respectively. In the first October days, the coastline retreated 7 m between in the N-camera zone and 15 m in the NW-camera zone to a level similar to May, before the nourishment took place.

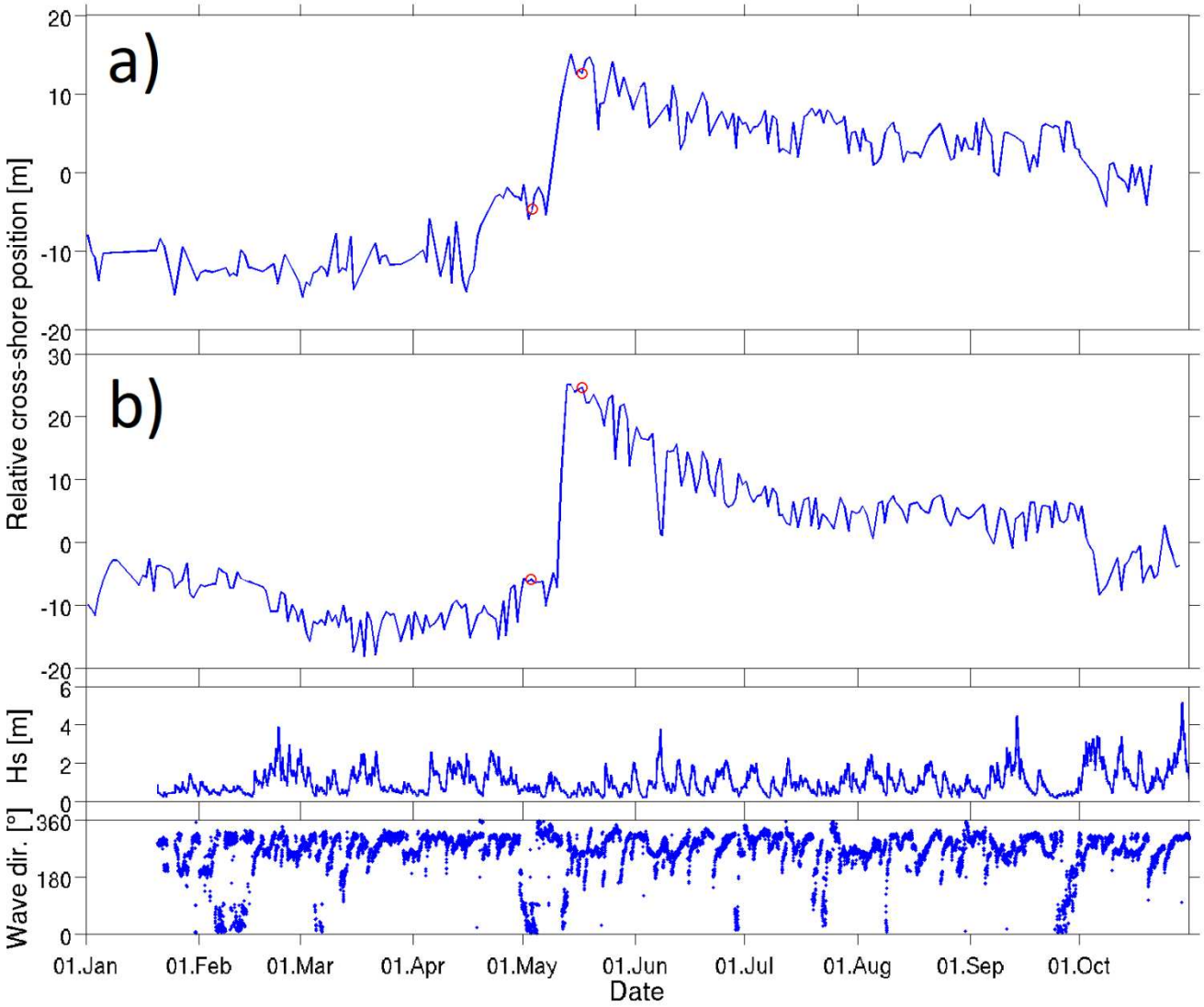

Fig. 7. Averaged coastline positions of a) the southern part of the N-camera (100-730 m north of the camera system) and b) the NW-camera (0-480 m). Values are plotted in relation to the all-time mean position of the respective beach section. Red circles: Dates of the terrestrial topography measurements. Additionally shown are the significant wave height and mean direction of incoming waves, measured at the Westerland buoy (BSH).

4 Discussion

4.1 Seasonal Morphology Variations

The natural variation of the averaged coastline position of more than 20 m and the variability of geomorphological elements reveals the highly dynamic morphology of Sylt's west coast (see also Blossier et al. 2017b). This variation of the coastline position displays the change between a winter beach and summer beach profile, due to the change from an erosive stormy wave climate in autumn and winter to a constructive low energy wave climate in spring and summer with a net landward sediment transport. The month with the most seaward coastline is also the month with the calmest wave climate with wave heights not exceeding 1.5 m (for wave heights see e.g. Fig. 4). Contradicting, in April beach broadening occurred during days with relative high wave climate. No nourishments took place at Sylt's beach before the 30th of April in 2017. The fact, that the broadening set in first in

the most northern part of the observed beach and moved southward points to a sediment input via the southward coast parallel current from the north.

The morphological changes also show a clear change between winter and summer in the distinct beach states following the definition from Wright and Short (1984). The observed winter morphology with its weak undulation and the continuous coast parallel sandbars, separated by a runnel from the beach, matches the intermediate ridge-and-runnel beach state. The strong undulation, developing in spring, together with the now frequently appearing skewed rip channels, mostly being in line with the beach embayments, correspond to the skewed-transverse-bar-and-rip beach state. The latter beach state usually develops during constructive beach growth phases, which is conform with the observed simultaneous beach broadening in Spring.

We noticed southward migration of about 100-200 m of the rip channels and aligned beach embayments in spring with merging beach horns and a set in of northward migration beginning in mid-September. This migration was also observed by Blossier et al. (2017a), who observed the Bunker Hill beach from 2011 until 2014. They found that the covered distances between winter and summer amounted to 200-300 m. The causes for this coast parallel migration are not yet fully understood but are likely linked to the seasonal variations in wave climate.

4.2 Beach Nourishment Observation

The constant video monitoring allowed for a detailed observation of the beach nourishment executed in May 2017. It showed that the nourishment was successful and initially broadened the local beach by more than 30 m. The immediate set in of redistribution of the supplied sand occurred, as the new beach morphology was forced to its new equilibrium state (Dean 1991). The beach slope was flattened, indicated by the MWL coastline retreat and simultaneous seaward migration at 1 m below. The coast parallel sediment movement 200 m to the north and an unspecified distance to the south additionally added to the redistribution. A new equilibrium state was reached after 1.5 months by the end of June. After the redistribution to the new equilibrium state, the beach still was 10 m broader than before the nourishment until end of September. The separation of the northern part of the undulation crest of the supplied sand body beginning in end of June probably follows a reshaping to the wave enforced undulation pattern along the beach. Blossier et al. (2017a) also observed that a part of a nourishment sand body separated and probably merged with an existing undulation crest in the north. Anyhow, early in October, the coastlines retreated to a level before the nourishment: The supplied sand got entirely eroded. The beach nourishment thus lasted 5.5 months. The cause of the erosion was the very high energetic wave climate from the 1st until the 8th of October. During that time, the significant wave height in the German Bight stayed constantly above 1.5 m. Peaks reached up to 3.4 m when the severe storm Xavier hit the German coast from the 4th until the 6th of October. The crucial factor for the beach erosion was probably not the high maximal wave heights, but the long duration. This statement is concluded from a comparison with several storms, which had occurred previously during the observation. The previous storms lead not to persistent coastline retreat at Bunker Hill beach, even so significant wave heights were even higher. For example, during the storm Sebastian on the 13th of September significant wave heights reached up to 4.5 m, but no coastal retreat occurred.

5 Conclusion

We showed how well natural morphology variations and beach nourishments can be monitored over long-time durations (in this case over 304 days), with resolutions that can keep up with costly and time-consuming alternative measuring campaigns.

Seasonal coastline migrations of up to 22 m and even distinct beach state transformations between deconstructive winter and constructive summer wave climates could be detected. Effects of occurring storms were determined. Considering the observed southward migration of the rip channels and aligned beach embayments in spring with merging beach horns, the fact that this phenomenon was also observed during the study from Blossier et al. (2017a), show that it is consistent over years.

The observed beach nourishment was successfully evaluated, determining the resulting beach broadening, the sand redistribution to a new equilibrium state and finally the erosion due to storm Xavier.

References

Blossier, B., Bryan, K. R., Daly, C. J., Winter, C., 2017a. Spatial and temporal scales of shoreline morphodynamics derived from video camera observations for the island of Sylt, German Wadden Sea. Geo-Marine Letters, Springer, 37 (2), 111–123.

Blossier, B., Bryan, K. R., Daly, C. J., Winter, C., 2017b. Shore and bar cross-shore migration, rotation and breathing processes at an embayed beach. Journal of Geophysical Research: Earth Surface, John Wiley & Sons, *122* (10), 1745-1770.

Dean, R. G., 1991. Equilibrium beach profiles: characteristics and applications. Journal of coastal research, Coastal Education & Research Foundation, 7 (1), 53–84.

Heikkila, J., Silven, O., 1997. A four-step camera calibration procedure with implicit image correction. IEEE Computer Society Conf. Computer Vision and Pattern Recognition, 1106–1112.

Klatt, E., 2013. Sylt - Geologie einer Nordseeinsel. Wachholtz; Neumünster.

Mapmaker.nationalgeographic.org. 2019. NatGeo Mapmaker Interactive. [online] Available at: http://mapmaker.nationalgeographic.org/zyUPgeeUlixlZ9nnTOpeG/ [Accessed 12 May 2019].

Richter, A., Faust, D., Maas, H.-G., 2013. Dune cliff erosion and beach width change at the northern and southern spits of Sylt detected with multi-temporal Lidar. Catena, Elsevier, 103, 103–111.

Smith, R., Bryan, K., 2007. Monitoring beach face volume with a combination of intermittent profiling and video imagery. Journal of Coastal Research, Coastal Education & Research Foundation, 23, (4), 892–898.

Tillmann, T. & Wunderlich, J. 2014. Barrier spit accretion model of Southern Sylt, German North Sea: Insights from ground-penetrating radar surveys and sedimentological data. Zeitschrift für Geomorphologie, Supplementary Issues, Borntraeger, 58 (3), 137–161.

Wright, L., Short, A., 1984. Morphodynamic variability of surf zones and beaches: a synthesis. Marine Geology, Elsevier, 56 (1-4), 93–118.

Woodroffe, C. D., 2002. Coasts: form, process and evolution. Cambridge University Press, Cambridge.